Korea-Australia Rheology Journal, 28(3), 197-205 (August 2016) www.springer.com/13367
DOI: 10.1007/s13367-016-0020-9

Comparison of rheological behaviors with fumed silica-based shear thickening fluids

Alain D Moriana[1], Tongfei Tian[2], Vitor Sencadas[1] and Weihua Li[1,*]
[1]*School of Mechanical, Materials and Mechatronics Engineering, University of Wollongong, Wollongong NSW 2522, Australia*
[2]*Intelligent Fluid Control Systems Laboratory, Institute of Fluid Science, Tohoku University, 2-1-1 Katahira, Aoba-ku, Sendai 980-8577, Japan*

(Received January 12, 2016; final revision received April 25, 2016; accepted July 8, 2016)

Shear thickening fluids (STFs) of differing compositions were fabricated and characterised in order to observe the effect of varying chemical and material properties on the resultant rheological behavior. Steady shear tests showed that for a given carrier fluid and particle size exists an optimum weight fraction which exhibits optimal shear thickening performance. Testing also showed that increasing particle size resulted in increased shear thickening performance and its onset whilst altering the carrier fluid chemistry has a significant effect on the thickening performance. An explanation is provided connecting the effect of varying particle size, carrier fluid chemistry and weight fraction to the resultant rheological behavior of the STFs. Two STFs were chosen for further testing due to their improved but contrasting rheological behaviors. Both STFs displayed a relationship between steady and dynamic shear conditions via the Modified Cox-Merz rule at high strain amplitudes ($\gamma_0 \geq 500\%$). Understanding the effects of particle and liquid polymer chemistry on the shear thickening effect will assist in 'tailoring' STFs for certain potential or existing applications.

Keywords: shear thickening fluids, rheological properties, viscosity, fumed silica, Cox-Merz rule

1. Introduction

Shear thickening fluids (STFs) are a relatively new polymeric material that exhibits non-Newtonian behavior in which the viscosity of non-Newtonian fluids is dependent on the applied shear rate. STFs are unique as the viscosity of the solution increases with increasing shear rate, when a certain shear rate is applied, in a phenomenon known as "Shear Thickening". Specifically, above a critical shear rate, the viscosity of the STF exponentially increases with increasing shear force, often described as the "Shear thickening effect". Another unique aspect is the reversibility of this effect as the STFs will return to fluid state once the shear force is removed or reversed, making it advantageous as a reusable product in applications. Current applications with STFs include scenarios which require energy adsorption from sharp projectiles such as knife or spike attacks (Gong *et al.*, 2014; Hassan *et al.*, 2010; Lee and Kim, 2012; Lee *et al.*, 2003; Li *et al.*, 2013; Petel *et al.*, 2013; Srivastava *et al.*, 2012; Wetzel *et al.*, 2004; Zhao *et al.*, 2012a; Zhao *et al.*, 2012b), acoustic and mechanical vibrational dampening control (Fischer *et al.*, 2006; Neagu *et al.*, 2009) and in a passive capacity in other polymeric materials (Jiang *et al.*, 2014; Peng *et al.*, 2014; Zhang *et al.*, 2010). The theory of shear thickening includes an order-disorder transition of particles (Hoffman, 1972; 1974) and formation of clusters, otherwise known as "hydroclusters" (Bergenholtz *et al.*, 2002; Boersma *et al.*, 1995; Durlofsky *et al.*, 1987; Lee *et al.*, 1999) that only form once the applied shear forces overcome particle repulsion forces.

Current research shows a gap in understanding the relationship between the rheological behavior of STF and their resultant effect in practical applications such as impact adsorption. It is crucial to understand the effect of systematically changing material properties on the STF's resultant rheology in order to manufacture a STF that suits the required application. A STF that thickens at very low shear stresses would be useful in sensitive applications such as acoustic dampening or low impact situations whilst a STF that thickens at higher shear stresses would be optimally used in high impact scenarios such as ballistic impacts. Barnes (1989) gathered that the particles within a STF governed its rheological response and the shape, size, surface chemistry, volume fraction, dispersion in medium and reaction with the liquid all affected the STF's rheological properties. Ideally, by quantifying the effects of changing each variable on the resultant rheology, STFs can be fabricated to suit a certain application by simply altering its composition. In the present work, several STFs were produced from polyethylene glycol (PEG) and polypropylene glycol (PPG) with three different sized fumed silica particles at a range of weight fractions in the final STF. Rheological properties of the different samples were systematically characterised in order to determine the effect of varying certain material properties and their

*Corresponding author; E-mail: weihuali@uow.edu.au

resultant rheological behavior. Theories as to how the varying material properties affect the formation of hydro-clusters under steady shear were postulated.

2. Experimental

2.1. Materials

Three types of fumed silica were used in this experiment: AEROSIL® 130 (A130), AEROSIL® 90 (A90) and AEROSIL® OX 50 (OX50) which were all supplied by EVONIK Industries AG. All fumed silica particles were hydrophilic in nature, sensitive to moisture adsorption. The materials properties for all fumed silica variants can be viewed below in Table 1. Before preparation, the fumed silica was place in a vacuum chamber for 24 h and heated to 110°C to eliminate any moisture. PEG was used as carrier fluid with molecular weights of 400 g/mol. PPG was supplied in two differing molecular weights, 400 and 725 g/mol. All carrier fluids were supplied by Sigma-Aldrich. The main properties of PEG and PPG are presented in Table 2.

2.2. STF fabrication processing

For each STF, certain amounts of fumed silica were added to the various carrier fluid with a certain weight fraction (from 20 wt.% to 55 wt.%). The silica was mixed with carrier fluid, by hand, until it was apparent all fumed silica particles were satisfactorily blended into the carrier fluid in order to ensure an enhanced mixture of particles within the fluid. Once mixed, the mixture was placed in a vacuum chamber for one hour to remove any trapped air bubbles, then an additional mechanical stirring step was requested to ensure adequate distribution of silica within the STF.

2.3. Materials characterization

Testing was completed with a parallel-plate Rheometer (MCR 301, Anton Paar, Germany) under steady shear and dynamic conditions with increasing angular frequency. A 20 mm diameter testing geometry (PP-20) was used with a gap of 0.8-1.0 mm to ensure adequate filling of the STF over the testing disk. Viscosity was measured as a function of shear rate within the range of 0.1-1000 s^{-1} at 20°C.

Table 1. Material properties of A130, A90 and OX50.

Particle name	Primary particle size (nm)	BET-surface area (m^2/g)	Tapped density (g/l)
A130	16	130±25	50
A90	20	90±15	80
OX50	40	50±15	130

Provided by the supplier.

Table 2. Material properties of PEG400, PPG400 and PPG725

Polymer name	Molecular weight (g/mol)	Degree of polymerisation	Density at 25°C (g/mL)
PEG400	400	9.09	1.13
PPG400	400	6.90	1.01
PPG725	725	12.50	1.01

3. Results and Discussion

3.1. Characterization of STF mixtures

Fumed silica was chosen for testing due to its ability to induce shear thickening at relatively lower weight fractions compared with spherical silica and its increased particle-particle repulsion forces which lead to increased dispersion within the carrier fluid (Raghavan and Khan, 1997). Transmission Electron Microscopic (TEM) images were taken for both fumed silica batches and are shown in Fig. 1.

Preliminary testing was completed on various wt.% of both fumed silica batches in PEG400 and PPG400 to determine the optimum weight fraction of each batch that exhibit the highest shear thickening behavior. Fumed silica particles A90 was blended with PEG400, PPG400 and PPG725 in weight fractions between 20-40 wt.% and the resultant steady shear test results are shown below in Fig. 2.

At low shear rates ($\dot{\gamma} < 1\ s^{-1}$) all mixtures show shear thinning behavior which is characterised by decreasing viscosity with increasing shear rate. The onset of shear thickening at the critical shear rate, $\dot{\gamma}_c$, is an important point as it signifies the shear rate at which STF begins to thicken. Another important indication of the STF's ability to thicken is the ratio of the maximum viscosity to the viscosity at $\dot{\gamma}_c$, henceforth named 'Shear thickening ratio' (STR). With increasing wt% in PEG400 + A90, different rheological behaviors are observed as $\dot{\gamma}_c$ and STR increases when comparing 20% and 25% STFs. At 30%, there is a small increase in viscosity and overall shear thinning effect was observed, which is indicative of particle clustering, similar to that of a three dimensional network of an elastomer or gel. This was considered to be an

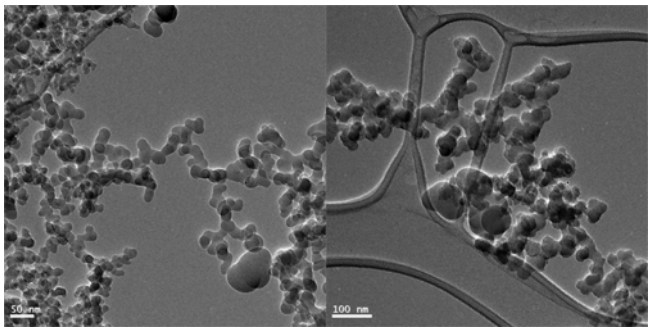

Fig. 1. Representative TEM images of AEROSIL® 90 (Left) and AEROSIL® OX 50 (Right).

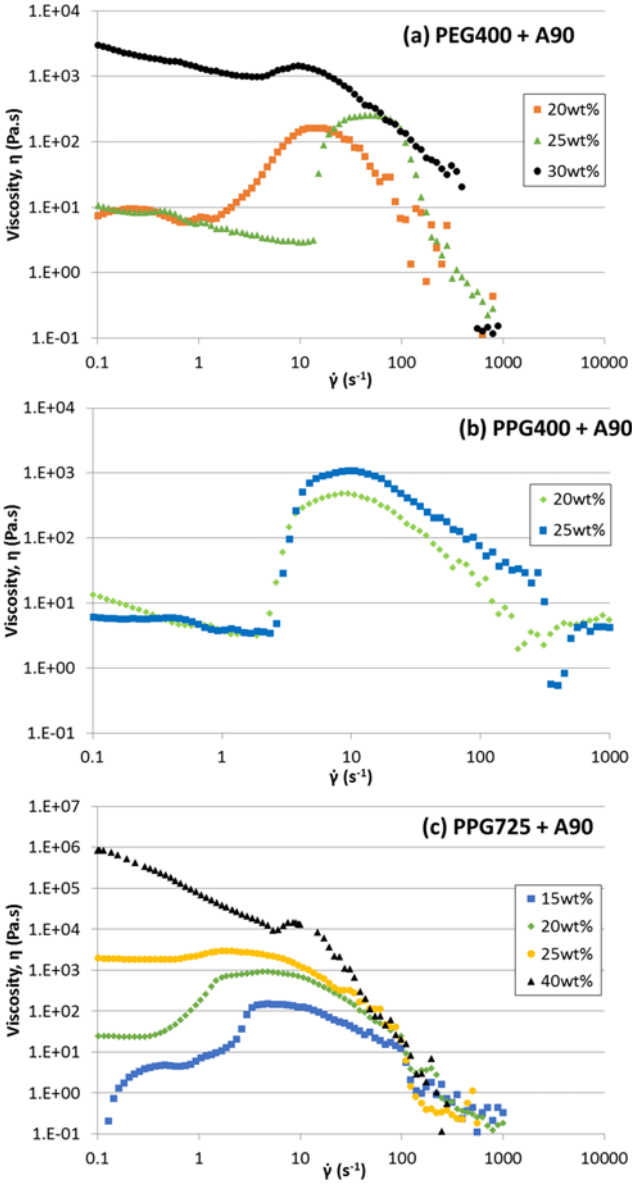

Fig. 2. (Color online) Viscosity measured as a function of shear rate under steady shear conditions for STF containing (a) PEG400 + A90, (b) PPG400 + A90 and (c) PPG725 + A90.

oversaturated STF (Fig. 2a).

In PPG400 + A90 (Fig. 2b), increasing the weight fraction shows significant increase in STR with infinitesimal change in $\dot{\gamma}_c$ and relatively larger in magnitude when compared to PEG400 + A90. We infer that the carrier fluid has a significant influence on the rheological properties of the STF when using the same fumed silica with same fractions. This is also evident when comparing 25 wt.% A90 fumed silica in three different carrier fluids shown in Fig. 3.

Increasing the molecular weight of PPG shows a predominately shear thinning mixture. A possible explanation is that the larger polymer chain of the PPG725 can result

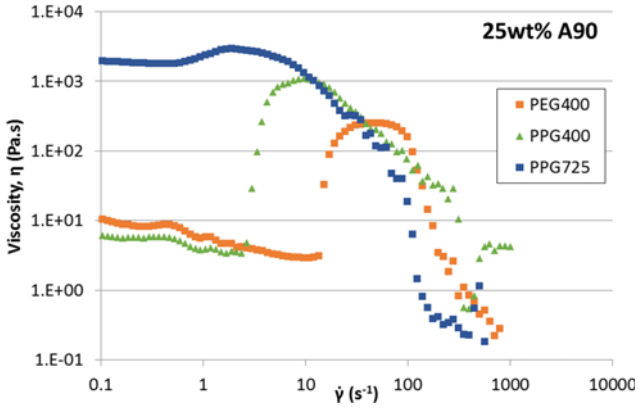

Fig. 3. (Color online) Viscosity measured as a function of shear rate under steady shear conditions for STF containing 25 wt.% A90 using different carrier fluids.

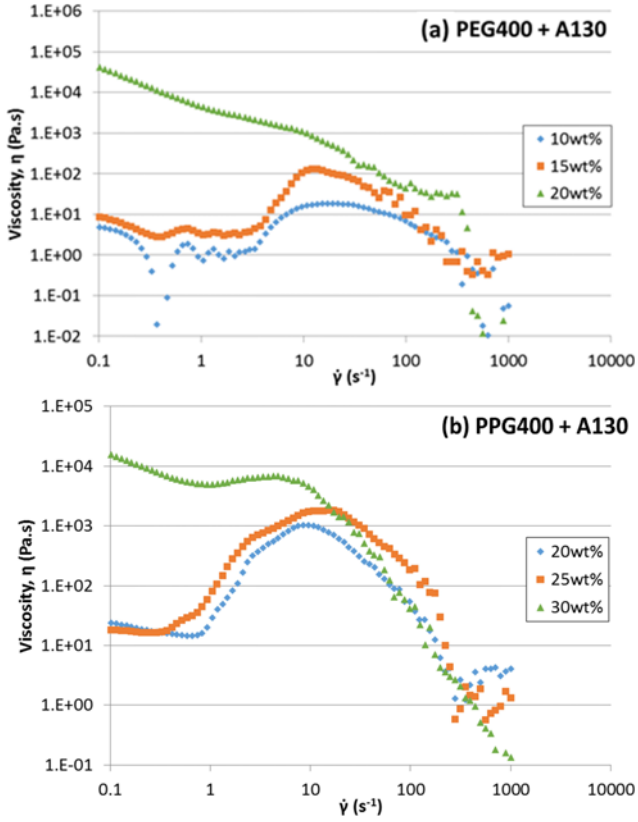

Fig. 4. (Color online) Viscosity measured as a function of shear rate under steady shear conditions for STF containing (a) PEG400 + A130 and (b) PPG400 + A130.

in entanglement with other PPG polymer chains within the solution, resulting in overall increased viscosity and difficulty to rearrange themselves under low to medium shear rates. As a consequence, STFs containing PPG725 were not further explored due their poor behavior as a possible application.

STF mixtures containing A130 were then mixed into

PEG400 and PPG400 at varying weight fractions. The results are shown in Fig. 4. The rheological behaviours are significantly different when compared to using A90 fumed silica. For instance, the shear thickening phenomenon was observed in PEG400 + A130 at lower weight fractions and gel-like behaviour occurred at 20 wt.%. Although the shear thickening effect was relatively poorer in PEG400 + A130 mixtures, fewer particles were required to observe this effect. In mixtures containing PPG400 + A130, the shear thickening effect was considerably unstable and the increase in viscosity past $\dot{\gamma}_c$ increased gradually and not sharply as observed in other STFs. The decreased particle size of A130 has a significant effect on the thickening effect of STFs. Wang and Wunder (2000) quantified the differences of two types of fumed silica sizes and observed that "state of aggregation/agglomeration therefore increases with decreasing particle size". Gun'ko *et al.* (2005) also stated that the aggregation of primary particles decreases with decreasing specific surface area. Increased degrees of aggregation in smaller particles are proportional to increased aspect ratios and increased chances of interparticle clustering or 'hooking' to form a three-dimensional or 'gel' network. Gel-like behaviour typically exhibit a constantly

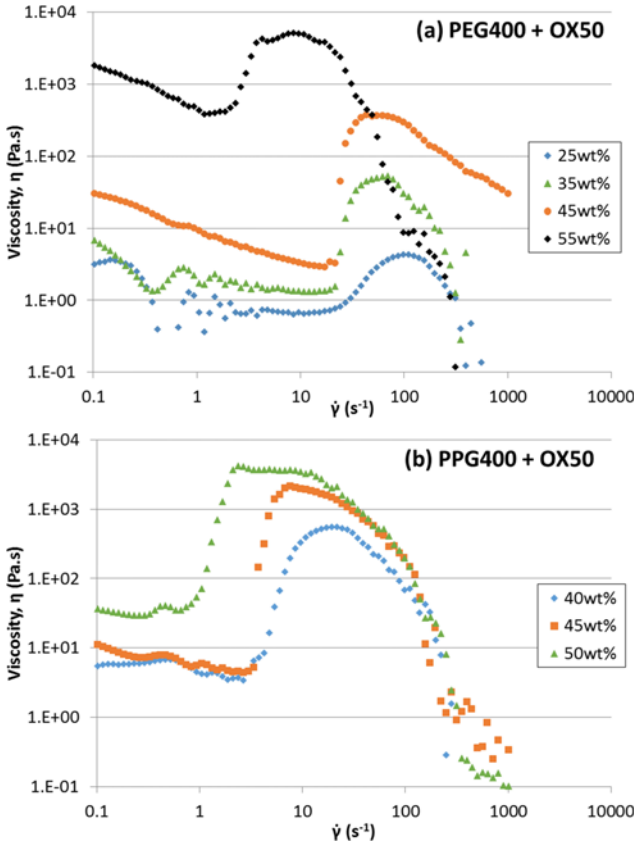

Fig. 5. (Color online) Viscosity measured as a function of shear rate under steady shear conditions for STF containing (a) PEG400 + OX50 and (b) PPG400 + OX50.

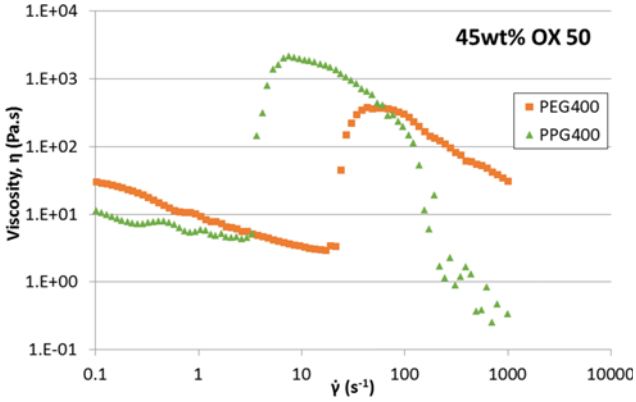

Fig. 6. (Color online) Viscosity measured as a function of shear rate under steady shear conditions for STF containing 45 wt.% OX50 using different carrier fluids.

shear thinning rheological response.

STF mixtures containing OX50 were then mixed into PEG400 and PPG400 at varying weight fractions and their resultant rheological behaviors are shown in Fig. 5. Similar trends found in the STFs containing A90 can also be seen in STFs containing OX50. In PEG400 + OX50 and PPG400 + OX50, the optimum weight fraction was found to be 45 wt.% which shows a good combination of $\dot{\gamma}_c$ and STR, increasing further resulted deterioration in performance, trending more to gel-like behavior (Fig. 5).

From these preliminary results; two STF mixtures were chosen based on their superior rheological behaviors: PEG400 + 45 wt.% OX50 and PPG400 + 45 wt.% OX50 henceforth known as STF_{PEG} and STF_{PPG} respectively (Fig. 6).

3.2. Discussion on variables and rheology of STF

Barnes (1989) stated that "All suspensions of solid particles will show the phenomenon [Shear thickening effect]". From this, we gather that the variables relating to particles including size, weight/volume fraction, surface chemistry and shape all have an effect on the resultant rheology when mixed with a fluid. To some extent, the reaction between the carrier fluid and the particles is also worth considering when attempting explaining the effect the relationship between physical variables and rheology. From this, a relationship can be developed that can quantify the effect of differing particle and carrier fluid material properties on the resultant rheological behavior of the STFs.

3.2.1. Weight fraction

During fabrication, the polymer chains within the carrier fluid react with the surface hydroxyl groups on the fumed silica (silanol groups) via hydrogen bonding. The resultant reactions between polymer and silica surface results in the formation of a layer of polymer surrounding fumed silica

called a "solvation layer" (Gun'ko *et al.*, 2005; Liu *et al.*, 2015; Raghavan and Khan, 1997; Raghavan *et al.*, 2000). This was initially proposed by Raghavan *et al.* (2000) in which they stated "in strongly hydrogen-bonding liquids, a solvation layer is envisioned to form on the silica surface through hydrogen bonding between liquid molecules and surface silanol groups.". The solvation layer was also used to explain the results found by He *et al.* (2015) when combining porous nanosilica particles in ethylene glycol. This hypothetical solvation layer around silica would increase interparticle distancing resulting in increased deflocculation and interparticle repulsion forces. By increasing weight fraction of fumed silica, there is a larger readily reactive silanol surface area. As shown in Figs. 3, 4, 5 and 6, there exists an optimum weight fraction of fumed silica, regardless of size, in which the shear thickening effect is pronounced. We suggest the remaining carrier fluid that has not reacted with the silanol surface groups act as lubrication between the fumed silica, allowing for increased particle distance and mobility to rearrange whilst under the applied shear force. Thus the conclusion can be made that a STF with a particle weight fraction below that of its optimum value will result in increased $\dot{\gamma}_c$ and decreased STR. This could be due to the larger interparticle distancing due to the abundance of unreacted liquid polymer chains present, requiring larger external forces to overcome this separation distance and the interparticle repulsion forces simultaneously. Inversely, by increasing the weight fraction beyond the optimum weight fraction, the STF is deprived of lubrication from unreacted polymer chains which results in creation of particle clusters, leading to complete disappearance of the shear thickening effect. This optimum weight fraction was more dependent on the size of the fumed silica and less on the chemistry of the carrier fluid. A graphical example of this theory can be seen in Fig. 8 where the critical shear rate and shear thickening ratio (η_{max}/η_c) were plotted against weight fraction. It is apparent that the critical shear rate of STFs containing PEG400 at varying weight fractions was significantly larger than STFs containing PPG400 and PPG725. PPG monomer has and additional methyl group in substitution of a hydrogen atom (Fig. 7), which increases the volume occupied by the PPG. When an external mechanical solicitation is applied to the polymer nanocomposite, the PEG carrier fluid can respond to those solicitations faster and leading to more packed particles within the fluid, when compared to the PPG. In this last carrier fluid, the size of

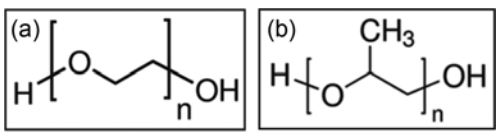

Fig. 7. (a) PEG and (b) PPG monomer unit.

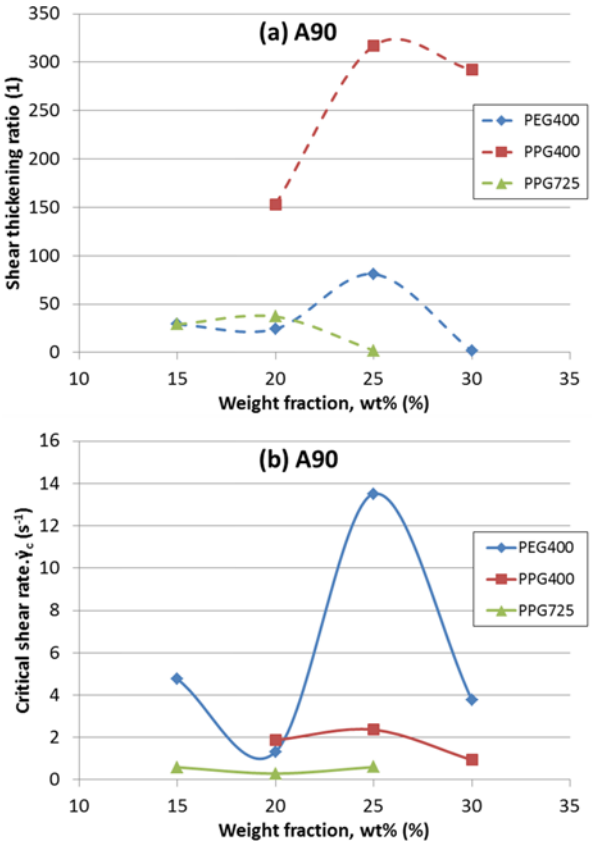

Fig. 8. (Color online) (a) Shear thickening ratio and (b) critical shear rate measured as a function of weight fraction mixed with A90 fumed silica under steady shear conditions.

the methyl groups hinders polymer accommodation of the carrier fluid, probably leading to a larger interparticle spacing.

3.2.2. Particle size

Comparing the material properties of A90 and OX50, the size of fumed silica is inversely proportional to its BET-surface area, which is indicative of the exposed silica surface area available to bond with the carrier fluid polymer chains. Also, the optimum weight fraction for STFs containing smaller fumed silica was found to be relatively lower than that for STFs containing larger fumed silica. This implies that an 'Effective surface area' exists in which particle separation and lubrication is at their most effective state. This is further supported as the optimum weight fraction of OX50 is almost twice that of A90, and almost three times that of A130 which also coincides with the surface area of OX50 almost halving that of A90 and a third of A130. A graphical demonstration can be seen in Fig. 9.

By increasing the particle size, we are able to increase the weight fraction before attaining this 'Effective surface area', allowing us to maximise weight fraction within the

STF, reduce interparticle distancing whilst allowing for sufficient space for particle rearrangement under shear stress. This would result in a higher shear thickening effect and lower $\dot{\gamma}_c$ due to the reduced external forces required to overcome particle repulsion forces. Another interesting relation is the effect of increasing particle size resulted in overall increased shear thickening performance and increased critical shear rate values.

In terms of potential applications, using larger particles will amplify the shear thickening effect and critical shear rate at the compromise of using more particles. By analyzing the requirements of the STF in mechanical applications, a suitable STF mixture can be fabricated that satisfy the application's thickening requirements and the shear force range at which it occurs.

3.2.3. Carrier fluid chemistry

Observing the effect of varying liquid chemistry with equivalent molecular weight (PEG400 vs. PPG400) was explored experimentally. With PPG400, the shear thickening effect was found to occur at lower shear rates and at significantly larger magnitudes than PEG400. It was also observed that there was very little change in $\dot{\gamma}_c$ with changing weight fraction in PPG400 (Fig. 8).

A possible theory as to why STFs with PPG attain shear thickening sooner is the relatively smaller DP which could affect the thickness of the solvation layer formed around the particles in the STF. This can attribute to smaller interparticle distancing and weaker particle-particle repulsion which results in less external force required for initiating shear thickening. Another possible suggestion is the composition of PEG compared to PPG. The only difference between these two polymers is an additional methyl branch within the PPG monomer, resulting in more rigid behavior under flow. More rigid polymer chains can typically lead to increased spacing between adjacent chains and reduced entanglement allowing for easier rearrangement whilst under shear flow. Therefore, ease of polymer flow will result in easier particle rearrangement to attain the shear thickening effect at lower shear rates. Comparing both STF mixtures with differing carrier fluids as shown in Fig. 6, a similar trend is observed in which the rheological response of STFs containing PPG400 shows lower $\dot{\gamma}_c$ but higher STR and vice versa for STFs containing PEG400. Another interesting observation is the equal optimum weight fractions observed in both PEG400 and PPG400. The difference in rigidity of the carrier fluid chemical composition has little effect on the 'effective surface area' at which the same amount of particles added to both PEG400 and PPG400 will exhibit the maximum shear thickening effect and $\dot{\gamma}_c$ of both STFs.

Comparing carrier fluids with similar chemical composition but with varying molecular weights (PPG400 vs. PPG725) in Fig. 8 showed that STFs with higher molecular weight carrier fluid resulted in significantly lower STR and lower optimum weight fraction. These findings are consistent with those reported by Xu *et al.* (2010). EG and PEG are commonly used in STF research and their mixtures with silica particles usually exhibit shear thickening when mixed with (Baird *et al.*, 2010; Hassan *et al.*, 2010; Lee *et al.*, 2003; Li *et al.*, 2013; Liu *et al.*, 2015; Petel *et al.*, 2013; Shan *et al.*, 2015; Xu *et al.*, 2010). The main difference differentiating PEG and EG is that PEG is a polymer of EG with a much higher degree of polymerization (DP) which could affect fluid viscosity. The molecular weight of a polymer is proportional to the DP, which could result in heavier polymer chains to form larger solvation layers on the particles, increasing interparticle distancing and repulsion forces. Another possible explanation is the increased DP resulted in entanglement, which hindered the formation of hydroclusters under shear stress. However, by observing Fig. 8b the $\dot{\gamma}_c$ of both PPG400 and PPG725 show minute changes. One could infer the effect of decreasing the molecular weight of the carrier fluid would increase the shear thickening effect while the shear rate at which thickening commences remains relatively stable.

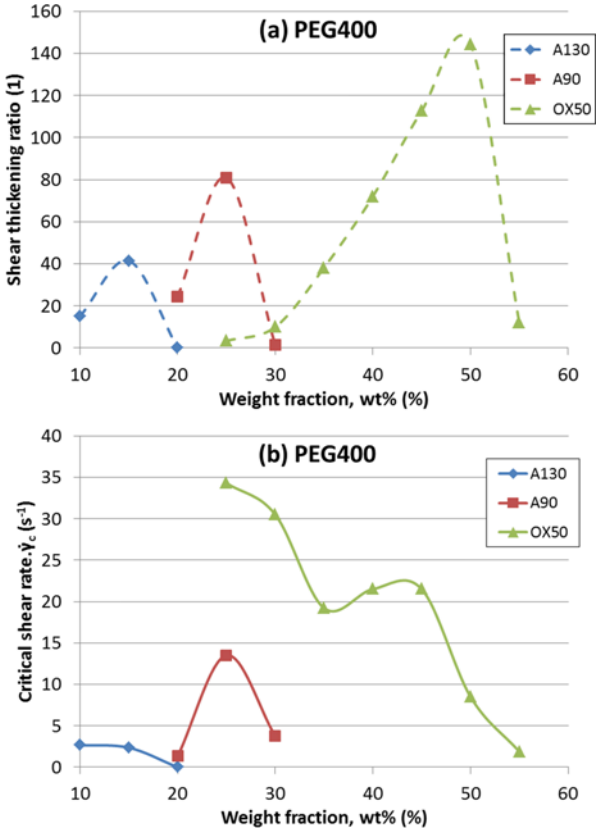

Fig. 9. (Color online) (a) Shear thickening ratio and (b) critical shear rate measured as a function of weight fraction mixed in PEG400 carrier fluid under steady shear conditions.

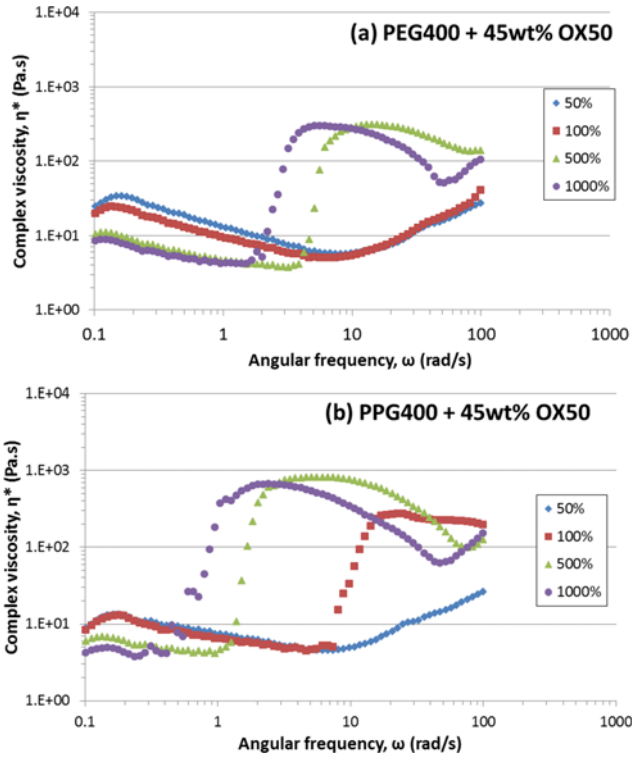

Fig. 10. (Color online) Dynamic frequency tests conducted on (a) STF_{PEG} and (b) STF_{PPG}. Each data series represents the strain amplitude (γ_0) applied.

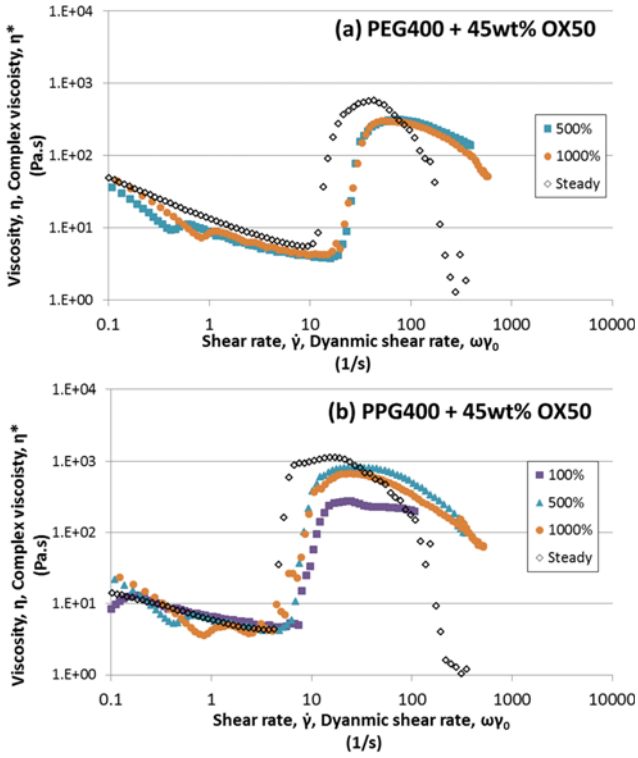

Fig. 11. (Color online) Correlation of steady and dynamic shear test data of (a) STF_{PEG} and (b) STF_{PPG} using MCM rule. Each data series represents the strain amplitude (γ_0) applied.

3.4. Validity with the Modified Cox-Merz Rule

Several previous investigations attempted to relate the shear thickening effect of STFs under steady shear conditions to those under dynamic (oscillatory) shear conditions using the Modified Cox-Merz theory (MCM) (Chellamuthu *et al.*, 2009; Fischer *et al.*, 2007; Galindo-Rosales *et al.*, 2009; Raghavan and Khan, 1997), mathematically represented as:

$$\eta(\dot{\gamma}) = \eta^*(\omega\gamma_0) \tag{1}$$

This relationship allows us to characterise a similar thickening effect under oscillatory shear flow, refereed as shear stiffening effect. Both STF_{PEG} and STF_{PPG} were tested under dynamic testing conditions. In which the amplitude shear strain, γ_0, is provided whilst the frequency is gradually increased. The results are shown in Fig. 10.

Under comparison, both STF_{PEG} and STF_{PPG} behave differently as they do under steady shear conditions. STF_{PEG} begins to show signs of shear stiffening when $\gamma_0 \geq 500\%$ whereas in STF_{PPG} shear stiffening is apparent at $\gamma_0 \geq 100\%$ which also shows a relative increase in the ratio of η^*_{max}/η^*_c. As observed previously, STF_{PPG} was observed to exhibit shear thickening at lower shear rates and greater magnitudes than STF_{PEG}, which also appears evidently under oscillatory condition. Further analysis was completed by calculating the dynamic shear rate ($\omega\gamma_0$) and comparing with steady shear results to observe the validity of the MCM rule (Fig. 11).

The MCM model applies to a limited extent in both STFs but only at higher strain amplitudes ($\gamma_0 \geq 500\%$). The dynamic shear data fits relatively well with the shear data as the deviation of $\dot{\gamma}_c$ with $\omega\gamma_0$ is relatively minor. The significance of these findings can allow for future research to extrapolate findings from steady shear tests to estimate the STF's shear stiffening performance under dynamic testing.

4. Conclusions

The effect of varying particle and liquid parameters on the resultant shear thickening effect was quantified. For each STF, there existed an optimum weight fraction that depended on the size of the fumed silica and larger particles resulted in the increased shear thickening effect and critical shear rate. The chemical properties of carrier fluids had a significant effect on the shear thickening properties by adjusting the critical shear rate and the shear thickening ratio. It was proposed that the mentioned variables affect the formation of solvation layer around the particles and interparticle distancing via polymer lubrication. Two STFs were selected for further testing based on their improved rheological behaviour to observe whether they conform to

the Modified Cox-Merz rule and relate steady shear and dynamic shear conditions. Both STFs conformed to the rule which showed a relationship between shear-thickening and shear-stiffening at high strain amplitudes ($\gamma_0 \geq 500\%$). These theories and suggestions into the effect of varying material properties on rheology aim at providing the ability to 'tailor' STFs for potential applications and future testing will be planned to observe the effect of differing critical shear rate and shear thickening ratios on current and potential real world situations.

Acknowledgments

The authors acknowledge AEROSIL® for supplying fumed silica samples for testing and Sigma-Aldrich® for supplying the various carrier fluids used for testing.

References

Baird, J.A., R. Olayo-Valles, C. Rinaldi, and L.S. Taylor, 2010, Effect of molecular weight, temperature, and additives on the moisture sorption properties of polyethylene glycol, *J. Pharm. Sci.* **99**, 154-168.

Barnes, H.A., 1989, Shear-thickening ("Dilatancy") in suspensions of nonaggregating solid particles dispersed in Newtonian liquids, *J. Rheol.* **33**, 329-366.

Bergenholtz, J., J.F. Brady, and M. Vicic, 2002, The non-Newtonian rheology of dilute colloidal suspensions, *J. Fluid Mech.* **456**, 239-275.

Boersma, W.H., J. Laven, and H.N. Stein, 1995, Computer simulations of shear thickening of concentrated dispersions, *J. Rheol.* **39**, 841-860.

Chellamuthu, M., E.M. Arndt, and J.P. Rothstein, 2009, Extensional rheology of shear-thickening nanoparticle suspensions, *Soft Matter* **5**, 2117-2124.

Durlofsky, L., J.F. Brady, and G. Bossis, 1987, Dynamic simulation of hydrodynamically interacting particles, *J. Fluid Mech.* **180**, 21-49.

Fischer, C., C.J.G. Plummer, V. Michaud, P.E. Bourban, and J.A.E. Månson, 2007, Pre- and post-transition behavior of shear-thickening fluids in oscillating shear, *Rheol. Acta* **46**, 1099-1108.

Fischer, C., S.A. Braun, P.-E. Bourban, V. Michaud, C.J.G. Plummer, and J.-A.E. Månson, 2006, Dynamic properties of sandwich structures with integrated shear-thickening fluids, *Smart Mater. Struct.* **15**, 1467-1475.

Galindo-Rosales, F.J., F.J. Rubio-Hernández, and J.F. Velázquez-Navarro, 2009, Shear-thickening behavior of Aerosil® R816 nanoparticles suspensions in polar organic liquids, *Rheol. Acta* **48**, 699-708.

Gong, X., Y. Xu, W. Zhu, S. Xuan, W. Jiang, and W. Jiang, 2014, Study of the knife stab and puncture-resistant performance for shear thickening fluid enhanced fabric, *J. Compos Mater.* **48**, 641-657.

Gun'ko, V.M., I.F. Mironyuk, V.I. Zarko, E.F. Voronin, V.V. Turov, E.M. Pakhlov, E.V. Goncharuk, Y.M. Nychiporuk, N.N. Vlasova, P.P. Gorbik, O.A. Mishchuk, A.A. Chuiko, T.V. Kulik, B.B. Palyanytsya, S.V. Pakhovchishin, J. Skubiszewska-Zięba, W. Janusz, A.V. Turov, and R. Leboda, 2005, Morphology and surface properties of fumed silicas, *J. Colloid Interface Sci.* **289**, 427-445.

Hassan, T.A., V.K. Rangari, and S. Jeelani, 2010, Synthesis, processing and characterization of shear thickening fluid (STF) impregnated fabric composites, *Mater. Sci. Eng. A-Struct. Mater. Prop. Microstruct. Process.* **527**, 2892-2899.

He, Q., X. Gong, S, Xuan, W. Jiang, and Q. Chen, 2015, Shear thickening of suspensions of porous silica nanoparticles, *J. Mater. Sci.* **50**, 6041-6049.

Hoffman, R.L., 1972, Discontinuous and dilatant viscosity behavior in concentrated suspensions. I. Observation of a flow instability, *J. Rheol.* **16**, 155-173.

Hoffman, R.L., 1974, Discontinuous and dilatant viscosity behavior in concentrated suspensions. II. Theory and experimental tests, *J. Colloid Interface Sci.* **46**, 491-506.

Jiang, J., Y. Liu, L. Shan, X. Zhang, Y. Meng, H.J. Choi, and Y. Tian, 2014, Shear thinning and shear thickening characteristics in electrorheological fluids, *Smart Mater. Struct.* **23**, 015003.

Lee, B.W. and C.G. Kim, 2012, Computational analysis of shear thickening fluid impregnated fabrics subjected to ballistic impacts, *Adv. Compos. Mater.* **21**, 177-192.

Lee, J.D., J.H. So, and S.M. Yang, 1999, Rheological behavior and stability of concentrated silica suspensions, *J. Rheol.* **43**, 1117-1140.

Lee, Y.S., E.D. Wetzel, and N.J. Wagner, 2003, The ballistic impact characteristics of Kevlar® woven fabrics impregnated with a colloidal shear thickening fluid, *J. Mater. Sci.* **38**, 2825-2833.

Li, X., H.L. Cao, S. Gao, F.Y. Pan, L.Q. Weng, S.H. Song, and Y.D. Huang, 2013, Preparation of body armour material of Kevlar fabric treated with colloidal silica nanocomposite, *Plast. Rubber Compos.* **37**, 223-226.

Liu, X.-Q., R.-Y. Bao, X.-J. Wu, W. Yang, B.-H. Xie, and M.-B. Yang, 2015, Temperature induced gelation transition of a fumed silica/PEG shear thickening fluid, *RSC Adv.* **5**, 18367-18374.

Neagu, R.C., P.E. Bourban, and J.A.E. Månson, 2009, Micromechanics and damping properties of composites integrating shear thickening fluids, *Compos. Sci. Technol.* **69**, 515-522.

Peng, G.R., W. Li, T.F. Tian, J. Ding, and M. Nakano, 2014, Experimental and modeling study of viscoelastic behaviors of magneto-rheological shear thickening fluids, *Korea-Aust. Rheol. J.* **26**, 149-158.

Petel, O.E., S. Ouellet, J. Loiseau, B.J. Marr, D.L. Frost, and A.J. Higgins, 2013, The effect of particle strength on the ballistic resistance of shear thickening fluids, *Appl. Phys. Lett.* **102**, 064103.

Raghavan, S.R. and S.A. Khan, 1997, Shear-thickening response of fumed silica suspensions under steady and oscillatory shear, *J. Colloid Interface Sci.* **185**, 57-67.

Raghavan, S.R., H.J. Walls, and S.A. Khan, 2000, Rheology of silica dispersions in organic liquids: new evidence for solvation forces dictated by hydrogen bonding, *Langmuir* **16**, 7920-7930.

Shan, L., Y. Tian, Y.G. Meng, and X.J. Zhang, 2015, Influences

of medium and temperature on the shear thickening behavior of nano fumed silica colloids, *Acta Phys. Sin.* **64**, 068301.

Srivastava, A., A. Majumdar, and B.S. Butola, 2012, Improving the impact resistance of textile structures by using shear thickening fluids: a review, *Crit. Rev. Solid State Mat. Sci.* **37**, 115-129.

Wang, R. and S.L. Wunder, 2000, Effects of silanol density, distribution, and hydration state of fumed silica on the formation of self-assembled monolayers of n-octadecyltrichlorosilane, *Langmuir* **16**, 5008-5016.

Wetzel, E.D., Y.S. Lee, R.G. Egres, K.M. Kirkwood, J.E. Kirkwood, and N.J. Wagner, 2004, The effect of rheological parameters on the ballistic properties of shear thickening fluid (STF)-Kevlar composites, *Materials Processing and Design: Modeling, Simulation and Applications NUMIFORM 2004*, Columbus, USA, 288-293.

Xu, Y.L., X.L Gong, C. Penga, Y.Q. Sun, W.Q Jiang, and Z. Zhang, 2010, Shear thickening fluids based on additives with different concentrations and molecular chain lengths, *Chin. J. Chem. Phys.* **23**, 342-346.

Zhang, X., W. Li, and X. Gong, 2010, Thixotropy of MR shear-thickening fluids, *Smart Mater. Struct.* **19**, 125012.

Zhao, J., H. Cao, X. Li, J. Wan, K. Wang, and J. Zhang, 2012a, Effect of SiO_2 particle size on stab resistant properties of STF/Kevlar composites, *Acta Mater. Compos. Sin.* **29**, 54-61.

Zhao, J., H. Cao, X. Li, J. Wan, K. Wang, and J. Zhang, 2012b, The stab resistant properties of Kevlar/STF composites, *Third International Conference on Smart Materials and Nanotechnology in Engineering*, Shenzhen, China, 84091L-84091L-8.